GSA Data Repository 2017138

Potassium rich magmatism from a phlogopite-free source

Yu Wang [a,*], Stephen F. Foley [a] and Dejan Prelević [b,c]

[a] *ARC Centre of Excellence for Core to Crust Fluid Systems/GEMOC; Department of Earth and Planetary Sciences, Macquarie University, NSW 2109, Australia*

[b] *Faculty of Mining and Geology, Belgrade University, Đušina 7, 11000 Belgrade, Serbia*

[c] *Institute of Geosciences, University of Mainz, Becherweg 21, Mainz 55099, Germany*

SUPPLEMENTARY FILE

This file contains three figures and six tables.

ANALYTICAL METHODS

Major elements: Whole-rock major element compositions of the phyllite and dunite were determined by X-ray fluorescence spectrometry (XRF) using a Philips MagiXPRO spectrometer on fused discs. Major element compositions of melts and minerals were obtained by CAMECA SX-100 electron microprobe (EMP) at the Department of Earth and Planetary Sciences, Macquarie University, with operating conditions of generally 15 kV accelerating voltage and 20 nA beam current. Counting times were 10 s for peaks, and 5 s for each background. The peaks were calibrated by measurements of standards (natural minerals and synthetic oxides). For mineral phases a beam diameter of 1 μm was used, which was increased to 5 μm for the analysis of quenched melt areas.

Trace elements: Trace elements were analysed by laser ablation-inductively coupled plasma-mass spectrometry (LA-ICP-MS) at Macquarie University. For phyllite and dunite, rock powders were melted to form glass beads without any fluxing agent on an iridium strip heater in an argon atmosphere and analyzed by laser sampling of the glasses. All analyses used 266 nm Nd-YAG laser coupled to an Agilent 7500ce ICP-MS. The laser was operated at a repetition rate of 5 Hz, with laser energy at the sample site of 5–6 J/cm2, allowing data collection from individual grains in polished thick sections (up to 80 μm thickness) for at least 40 s. Nitrogen was mixed with helium before ablated materials were introduced into the ICP-MS. Data were measured for 60 s plus 30 s background with beam sizes of 30 μm and 50 μm for most samples, 80 μm for some large-grained melt pools, 15 μm and 20 μm for a few small-grained accessory phases and melt samples from experiments. ^{29}Si and ^{44}Ca were used as the internal standards applying the Si and Ca concentrations previously determined by electron microprobe. For calibration, NIST SRM 610 was analysed at the beginning and after every 20 measurements on the unknown samples. The time-resolved signal was processed using the program GLITTER 4.4.1 (www.glitter-gemoc.com, Macquarie University), applying the preferred values for NIST SRM 610 reported in the GeoReM database (http://georem.mpch-mainz.gwdg.de/) (Jochum et al., 2011). Analytical uncertainty (one sigma) for a spot analysis or line scan was less than 10 %. During each run the basaltic USGS BCR-2G reference glass was analysed as an unknown to monitor accuracy and reproducibility of the analyses.

EXPERIMENTAL METHOD

All experiments were performed in a 0.5-inch piston-cylinder apparatus based on a modified Boyd-England design at Macquarie University (Boyd and England, 1960). Furnace

assemblies (12.7 mm diameter) were made of graphite with cylindrical talc outer sleeve and pyrex® inner sleeve and BN inserts. Temperatures were measured using Pt–$Pt_{90}Rh_{10}$ thermocouples and automatically controlled by an Electromax V single loop controller. Samples were welded into a 4 by 4 mm Ag_{70}/Pd_{30} capsule with a wall thickness of 0.2 mm, minimizing iron loss to the capsule. Experimental conditions were applied by first applying pressure, followed by heating until the desired pressure and temperature were reached. Run durations were up to 192 hours. Where present, melt remained free of quench crystallization. Recovered capsules were cut into two parallel to their axis and embedded into epoxy mounts for polishing. Melt proportions in all experimental runs were obtained by program ImageJ using SEM image and mass balance calculation.

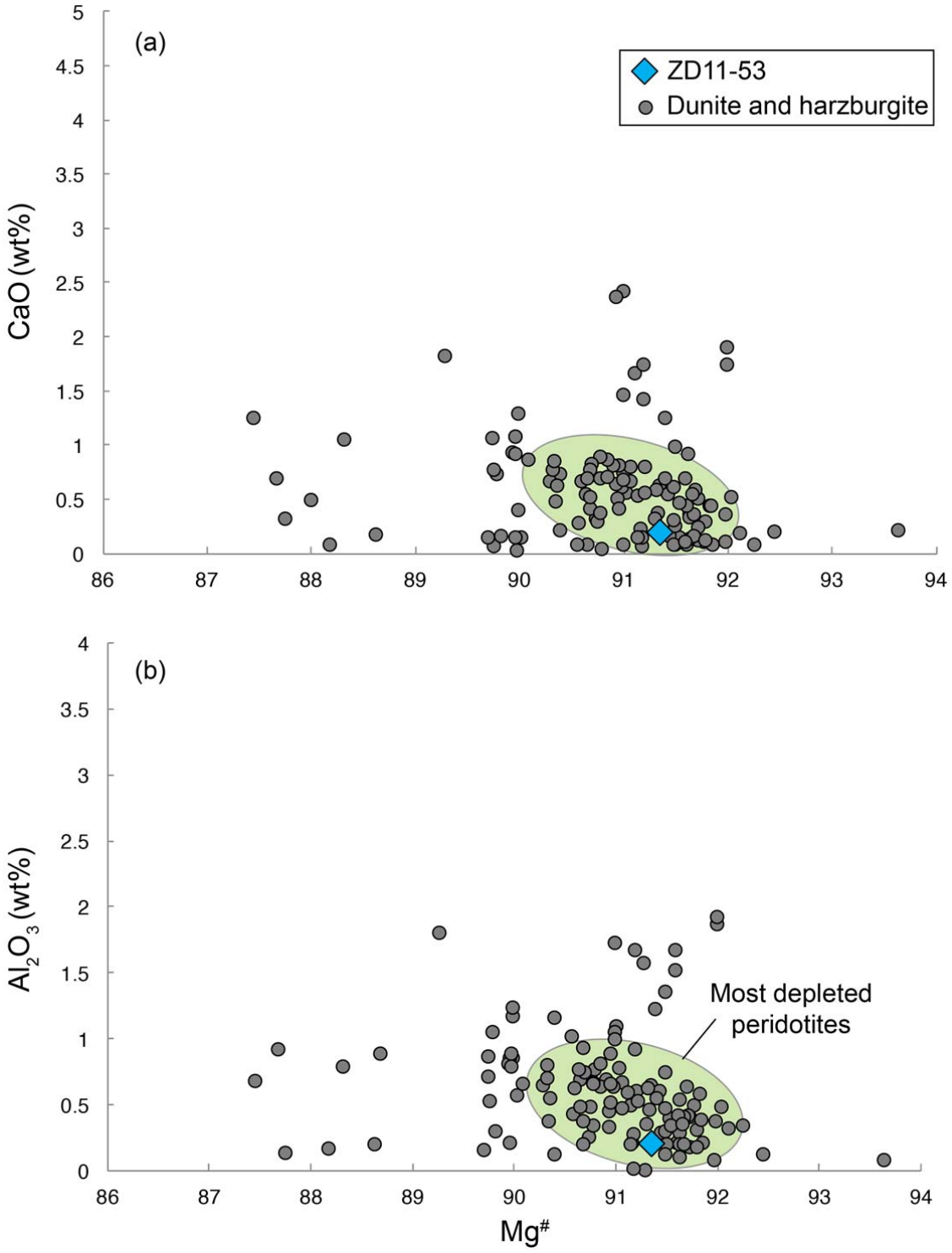

Fig. DR1 Compositions of $Mg^{\#}$ vs. (a) CaO (wt%) and (b) Al_2O_3 (wt%) of the dunite sample used in this study (ZD11-53) compared to natural depleted peridotites (Ishii et al., 1992; Parkinson and Pearce, 1998; Ohara and Ishii, 1998; Pearce, 1999; Khedr and Arai, 2010; Nozaka, 2014). $Mg^{\#}$ = 100*MgO/(MgO + FeO) in mole per cent.

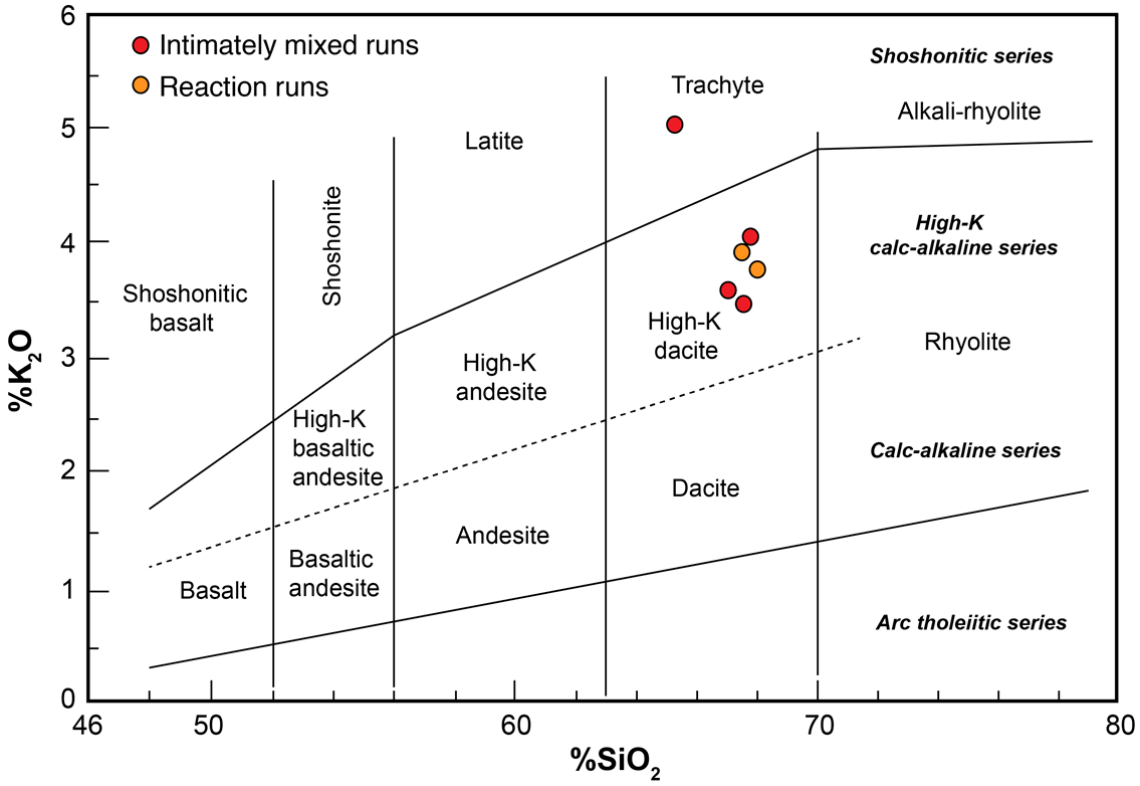

Fig. DR2 SiO_2 (wt %) vs. K_2O (wt %) classification plot for melts produced in this study. Adapted from Peccerillo & Taylor, 1976.

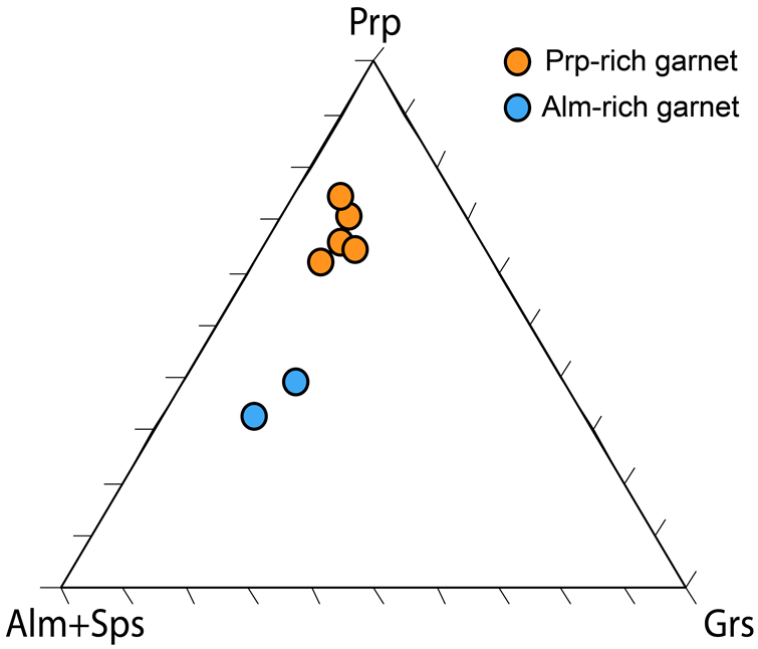

Fig. DR3 Ternary discrimination diagram of garnets produced from the experiments. Note the two compositionally different types. Prp: pyrope; Alm: almandine; Sps: spessartine; Grs: grossular.

TABLE DR1. MAJOR (WT%) AND TRACE (PPM) ELEMENT COMPOSITIONS OF STARTING MATERIALS

Locality	Kopaonik area, Serbia			Zedang area, South Tibet, China
Sample	11KP01			ZD11-53
Rock	Quartz-phyllite	GLOSS	UCC	Dunite
SiO_2	76.7	58.57	66	42.16
TiO_2	0.7	0.62	0.5	0.04
Al_2O_3	11.6	11.91	15.2	0.20
FeO_T	3.4	5.21	4.5	8.35
MnO	0.06	0.32	0.08	0.13
MgO	1.1	2.48	2.2	49.53
CaO	1.6	5.95	4.2	0.19
Na_2O	1.6	2.43	3.9	0.07
K_2O	1.9	2.04	3.4	0.00
Cr_2O_3	0.01	NA	NA	0.36
LOI	1.5			0.25
Sum	100.27			101.28
$Mg^{\#}$	37	46	47	91
Li	33	NA	20	2.2
Sc	13	13.1	13.6	4.0
Ti	4269	NA	2458	37
V	58	110	107	16
Cr	1362	78.9	83	1984
Mn	1147	NA	600	1011
Co	11	21.9	17	129
Ga	10	NA	17	0.43
Rb	54	57.2	112	0.003
Sr	288	327	350	0.30
Y	20	29.8	22	0.07
Zr	56	130	190	0.02
Nb	9.7	8.94	12	0.016
Cs	1.6	3.48	4.6	0.003
Ba	355	776	550	0.50
La	30	28.8	30	0.005
Ce	63	57.3	64	0.003
Pr	7.2	NA	7.1	0.001
Nd	28	27	26	0.003
Sm	5.6	5.78	4.5	0.001
Eu	1.1	1.31	0.88	0.001
Gd	4.6	5.26	3.8	0.003
Tb	0.68	NA	0.64	0.000
Dy	3.8	4.99	3.5	0.007
Ho	0.8	NA	0.8	0.002
Er	2.1	2.92	2.3	0.011
Tm	0.31	NA	0.33	NA
Yb	2	2.76	2.2	0.021
Lu	0.26	0.413	0.32	0.005
Hf	1.6	4.06	5.8	0.001
Ta	0.75	0.63	1.0	0.003
Th	8.4	6.91	10.7	0.001
U	1.5	1.68	2.8	0.008

Global Subducted Sediment (GLOSS) from Plank and Langmuir (1998); Upper Continental Crust (UCC) from Taylor and McLennan (1995) and McLennan (2001).

TABLE DR2. EXPERIMENTAL RUN CONDITIONS AND PRODUCTS.

Run No.	Geometry	P (GPa)	T (°C)	T_C (°C)	Hours	Phases (mode %)
2036	Reaction	2	1000	883	192	Dunite half: Ol (96), Cpx (2), *Chr* Phyllite half: M (42), Qrz (41), Alm-grt (12), Ky (2), *Zir, Apa, Rt* Interaction belt: Opx (2), *Prp-grt*
2037	Mixture	2	1000	933	192	Opx (75), M (23), Ol (5.5), *Chr, Prp-grt, Zir, Apa, Rt*
2038	Mixture	2	1100	942	168	Opx (71), M (28), *Chr*
139	Reaction	3	1000	1003	192	Dunite half: Ol (93), Chr (2), *Cpx* Phyllite half: M (31), Coe (44), Alm-grt (14), Ky (6), *Zir, Apa, Rt* Interaction belt: Opx (4), *Prp-grt*
140	Mixture	3	1000	871	192	Opx (71), M (14.5), Prp-grt (6), Coe (6), Cpx (1.5), *Zir, Chr*
141	Mixture	3	1100	936	168	Opx (66), M (18), Prp-grt (8), Coe (5), Cpx (2), *Zir, Chr*

Note: Phases in italics are accessory phases present in the run products in the range of 0-1 vol%. T_C denotes temperatures calculated by the two-pyroxene thermometer of Brey and Köhler, 1990, with error of ± 16°C. Mineral abbreviations: M, melt; Ol, olivine; Qrz, quartz; Alm-grt, almandine-rich garnet; Prp-grt, pyrope-rich garnet; Opx, orthopyroxene; Cpx, clinopyroxene; Chr, chromite; Coe, coesite; Ky, kyanite; Zir, zircon; Apa, apatite; Rt, rutile.

TABLE DR3. MAJOR ELEMENT COMPOSITIONS OF MELT (WT%)

Run No.	2036		2037		2038		139		140		141	
P (GPa)	2		2		2		3		3		3	
T (°C)	1000		1000		1100		1000		1000		1100	
Geometry	Reaction		Mixture		Mixture		Reaction		Mixture		Mixture	
N (Number of analyses)	10	1 SD	10	1 SD	11	1 SD	5	1 SD	5	1 SD	3	1 SD
SiO_2	68.54	0.80	67.16	0.49	67.89	0.33	68.21	0.73	68.46	0.68	65.50	0.87
TiO_2	0.53	0.02	0.64	0.02	0.79	0.02	0.39	0.01	0.54	0.01	0.62	0.04
Al_2O_3	15.84	0.52	14.88	0.41	14.44	0.09	14.21	0.42	13.15	0.10	13.33	0.16
Cr_2O_3	0.00	0.00	0.00	0.00	0.00	0.00	0.00	0.00	0.00	0.00	0.00	0.00
FeO	1.02	0.08	0.98	0.07	1.52	0.04	0.68	0.07	0.61	0.04	1.03	0.18
MnO	0.00	0.00	0.04	0.00	0.00	0.00	0.00	0.00	0.00	0.00	0.00	0.00
MgO	0.56	0.16	1.47	0.63	1.91	0.08	0.35	0.03	0.59	0.04	0.84	0.13
CaO	1.62	0.03	1.78	0.07	1.97	0.03	0.86	0.02	0.46	0.02	0.78	0.07
Na_2O	2.43	0.35	2.31	0.19	2.20	0.32	1.39	0.49	0.92	0.21	2.26	0.25
K_2O	3.84	0.11	3.52	0.11	3.38	0.13	4.08	0.38	4.22	0.46	5.09	0.49
Total	94.37		92.79		94.1		90.18		88.94		89.45	
Mg#	50		73		69		48		64		59	
A/(CNK)	1.43		1.37		1.33		1.72		1.90		1.25	
Degree of melting (%)	42		23		28		31		14.5		18	

Mg# = 100*MgO/(MgO + FeO) in mole per cent;
A/(CNK) = Aluminum saturation index, defined as the molecular ratio Al_2O_3 / (CaO + Na_2O + K_2O);
1 SD = one standard deviation, N refers to number of replicate analyses.

TABLE DR4. MAJOR ELEMENT COMPOSITIONS OF GARNET (WT%)

Run No.	2036				2037		139				140		141	
P (GPa)	2				2		3				3		3	
T (°C)	1000				1000		1000				1000		1100	
Geometry	Reaction				Mixture		Reaction				Mixture		Mixture	
N (Number of analyses)	3	1 SD	2	1 SD	6	1 SD	3	1 SD	2	1 SD	5	1 SD	11	1 SD
Type	Almandine-rich		Pyrope-rich		Pyrope-rich		Almandine-rich		Pyrope-rich		Pyrope-rich		Pyrope-rich	
SiO_2	39.41	1.06	41.31	0.34	41.61	0.58	38.49	0.26	42.33	0.64	42.32	0.78	42.60	0.99
TiO_2	1.11	0.24	1.05	0.26	0.91	0.37	1.27	0.42	0.73	0.42	0.81	0.05	0.60	0.32
Al_2O_3	22.33	0.16	22.95	0.04	22.17	0.72	21.33	0.56	22.26	0.01	22.50	0.56	22.95	0.89
Cr_2O_3	0.00	0.00	0.13	0.00	0.36	0.40	0.00	0.00	0.08	0.00	0.06	0.00	0.19	0.09
FeO	19.83	0.92	11.74	0.77	13.82	1.11	24.47	1.18	11.18	0.91	10.64	0.12	9.31	0.66
MnO	0.52	0.08	0.24	0.01	0.35	0.04	0.46	0.06	0.31	0.01	0.30	0.03	0.26	0.07
MgO	10.91	0.82	18.05	0.39	17.33	0.86	8.53	0.33	18.23	0.54	19.58	0.40	22.08	0.58
CaO	6.60	0.32	4.90	0.45	4.35	0.38	5.44	0.51	5.77	0.48	4.49	0.33	2.71	0.70
Na_2O	0.09	0.02	0.13	0.01	0.06	0.02	0.22	0.07	0.09	0.01	0.24	0.04	0.11	0.04
K_2O	0.05	0.02	0.00	0.00	0.06	0.00	0.04	0.01	0.03	0.00	0.08	0.01	0.05	0.01
NiO	0.00	0.00	0.00	0.00	0.05	0.00	0.00	0.00	0.00	0.00	0.06	0.00	0.06	0.00
P_2O_5	0.19	0.06	0.00	0.00	0.14	0.00	0.15	0.06	0.00	0.00	0.20	0.08	0.16	0.09
Total	101.1		100.5		101.2		100.4		101.0		101.3		101.1	
Pyrope	40%		64%		61%		32%		63%		68%		75%	
Almandine	41%		23%		27%		52%		22%		21%		18%	
Grossular	18%		12%		11%		15%		14%		11%		7%	
Spessartine	1%		0%		1%		1%		1%		1%		1%	

TABLE DR5. MAJOR ELEMENT COMPOSITIONS OF PYROXENES (WT%)

Run No.	2036		2037		2038		139		140		141		2036		139		140		141	
P (GPa)	2		2		2		3		3		3		2		3		3		3	
T (°C)	1000		1000		1100		1000		1000		1100		1000		1000		1000		1100	
Geometry	R		M		M		R		M		M		R		R		M		M	
N	5	1 SD	9	1 SD	10	1 SD	6	1 SD	11	1 SD	8	1 SD	3	1 SD	2	1 SD	4	1 SD	4	1 SD
Phase	opx		opx		opx		opx		opx		opx		cpx		cpx		cpx		cpx	
SiO_2	55.68	0.75	56.66	0.53	56.08	0.50	56.78	0.54	57.75	0.64	56.85	0.41	53.89	0.56	53.78	0.47	53.32	0.26	53.89	0.80
TiO_2	0.23	0.05	0.20	0.03	0.21	0.04	0.07	0.04	0.13	0.03	0.21	0.04	0.11	0.02	0.14	0.00	0.21	0.01	0.15	0.05
Al_2O_3	3.81	0.43	2.76	0.61	3.20	0.35	1.88	0.52	1.95	0.64	3.09	0.66	1.41	0.09	1.57	0.09	2.13	0.09	1.69	0.60
Cr_2O_3	0.10	0.04	0.15	0.07	0.21	0.09	0.39	0.28	0.00	0.00	0.07	0.02	0.64	0.20	0.83	0.13	0.80	0.01	0.53	0.38
FeO	6.70	0.72	7.32	0.47	7.11	0.46	6.63	0.81	6.32	0.86	6.12	0.51	2.02	0.03	2.63	0.52	2.05	0.08	1.99	0.11
MnO	0.10	0.01	0.12	0.01	0.12	0.01	0.14	0.03	0.08	0.02	0.09	0.02	0.05	0.01	0.10	0.04	0.05	0.00	0.06	0.00
MgO	32.82	0.90	32.07	0.79	31.92	0.61	33.50	0.72	33.12	0.53	32.54	0.88	17.34	0.20	17.62	0.60	16.49	0.08	16.95	0.44
CaO	0.42	0.12	0.53	0.18	0.56	0.10	0.60	0.14	0.21	0.07	0.44	0.23	24.52	0.68	23.23	0.88	24.57	0.16	24.40	0.46
Na_2O	0.05	0.01	0.09	0.03	0.11	0.03	0.11	0.10	0.21	0.12	0.31	0.12	0.30	0.12	0.34	0.07	0.36	0.06	0.37	0.12
K_2O	0.00	0.00	0.03	0.01	0.11	0.12	0.00	0.00	0.11	0.09	0.06	0.00	0.00	0.00	0.00	0.00	0.00	0.00	0.00	0.00
Total	99.91		99.93		99.62		100.1		99.88		99.79		100.28		100.22		99.96		100.02	
Wollastonite	1%		1%		1%		1%		0%		1%		48%		46%		49%		49%	
Enstatite	89%		87%		87%		88%		89%		89%		47%		49%		46%		47%	
Ferrosilite	10%		11%		11%		10%		10%		10%		3%		4%		3%		3%	
Aegirine/Acmite	0%		0%		0%		0%		1%		1%		1%		1%		1%		1%	

Note: R: Reaction; M: Mixture.

TABLE DR6. TRACE ELEMENT COMPOSITIONS OF MELT (PPM)

Run No.	2036		2037		2038		139		140		141	
P (GPa)	2		2		2		3		3		3	
T (°C)	1000		1000		1100		1000		1000		1100	
Geometry	R		M		M		R		M		M	
N	7	1 SD	6	1 SD	9	1 SD	6	1 SD	9	1 SD	8	1 SD
Li	86	6.3	33	1.9	42	2.9	82	4.7	26	3.1	23	2.2
Be	4.5	0.32	2.1	0.43	2.8	0.37	4.9	0.62	4.1	0.52	3.0	0.44
Sc	4.2	0.49	6.9	0.84	7.1	0.86	3.6	0.55	4.2	0.56	5.0	0.35
Ti	2950	138	2653	185	3654	277	2764	253	2574	304	3089	271
V	9.1	1.5	29	2.3	17	3.1	19	2.1	17	1.5	18	1.5
Cr	70	16	640	79	378	61	12	1.8	398	43	221	24
Mn	109	21	508	87	381	45	107	27	272	25	304	37
Co	3.6	0.61	43	8.6	27	2.8	2.7	0.38	25	3.1	21	2.4
Ni	7.9	1.2	708	82	287	39	155	24	479	45	243	31
Cu	2.8	0.44	1.2	0.31	2.1	0.27	3.0	0.39	5.7	0.57	2.0	0.38
Zn	21	3.8	25	3.2	17	1.9	31	4.0	50	4.4	10	1.5
Ga	23	2.0	9.3	1.5	9.2	1.2	27	2.6	23	2.7	14	2.1
Rb	167	9.1	99	8.9	119	23	206	14	219	29	191	16
Sr	294	16	167	13	209	24	346	25	336	37	341	37
Y	2.6	0.52	14	2.9	19	2.7	3.9	0.22	6.7	1.1	5.1	0.61
Zr	212	7.3	168	11	327	45	198	18	235	30	354	29
Nb	11	1.6	11	2.3	17	2.4	11	1.7	14	1.3	22	1.7
Cs	5.4	0.54	3.5	0.46	3.9	0.50	6.8	0.77	7.2	1.1	5.6	0.74
Ba	698	39	402	27	495	46	841	62	871	98	792	75
La	49	4.9	26	3.0	33	3.8	46	3.6	46	5.6	62	8.8
Ce	105	10	62	6.4	76	8.2	99	7.9	100	13	96	9.2
Pr	11	1.1	6.8	0.89	8.5	1.7	10	0.89	11	1.9	10	1.7
Nd	34	3.2	24	2.8	32	4.6	29	3.3	34	3.8	37	3.0
Sm	4.2	0.63	4.9	0.76	6.2	1.1	3.3	0.63	3.6	0.60	5.5	0.78
Eu	0.85	0.12	1.1	0.21	1.3	0.37	0.68	0.17	0.63	0.20	1.2	0.22
Gd	1.9	0.32	3.6	0.44	4.7	0.58	1.2	0.26	2.3	0.33	2.5	0.36
Tb	0.17	0.05	0.47	0.17	0.62	0.16	0.16	0.03	0.33	0.16	0.28	0.09
Dy	0.7	0.13	3.0	0.15	4.0	0.59	0.93	0.13	1.4	0.48	1.3	0.56
Ho	0.09	0.04	0.53	0.09	0.73	0.15	0.13	0.05	0.23	0.07	0.19	0.09
Er	0.17	0.09	1.6	0.32	2.0	0.47	0.47	0.04	0.58	0.12	0.41	0.12
Tm	0.03	0.01	0.18	0.05	0.25	0.03	0.10	0.03	0.10	0.05	0.06	0.03
Yb	0.17	0.06	1.2	0.24	1.6	0.34	0.55	0.08	0.56	0.09	0.31	0.06
Lu	0.02	0.01	0.12	0.03	0.27	0.04	0.10	0.02	0.1	0.03	0.07	0.01
Hf	6.3	0.78	4.0	0.66	8.4	1.1	4.8	0.69	6.0	0.77	8.8	0.78
Ta	1.1	0.22	0.93	0.23	1.4	0.29	1.0	0.09	1.4	0.17	1.9	0.23
Th	23	3.3	12	1.9	15	1.0	20	1.7	22	2.5	18	2.1
U	5.0	0.45	3.5	0.26	3.9	0.34	4.6	0.36	5.5	0.53	4.4	0.47
Th/La	0.47	0.08	0.46	0.09	0.45	0.06	0.43	0.05	0.48	0.08	0.29	0.05
Rb/Cs	31	3.5	28	4.5	31	7.1	30	4.0	30	6.1	34	5.3
Sm/La	0.09	0.02	0.19	0.04	0.19	0.04	0.07	0.01	0.08	0.02	0.09	0.02
Sr/Nd	8.6	0.94	7.0	0.98	6.5	1.2	12	1.6	9.9	1.6	9.2	1.2
Nb/Ta	10	2.5	12	3.8	12	3.0	11	2.0	10	1.5	12	1.7
Zr/Hf	34	4.3	42	7.5	39	7.4	41	7.1	39	7.1	40	4.9

Note: N: number of analyses; R: Reaction; M: Mixture.

REFERENCES

Boyd, F. R., and England, J. L., 1960, Apparatus for phase-equilibrium measurements at pressures up to 50 kilobars and temperatures up to 1750°C: Journal of Geophysical Research, v. 65, no. 2, p. 741-748.

Brey, G. P., and Köhler, T., 1990, Geothermobarometry in Four-phase Lherzolites II. New Thermobarometers, and Practical Assessment of Existing Thermobarometers: Journal of Petrology, v. 31, no. 6, p. 1353-1378.

Ishii T., Robinson P. T., Maekawa H. and Fiske R., 1992, Petrological studies of peridotites from diapiric serpentinite seamounts in the Izu-Ogasawara-Mariana forearc, Leg125. Proceedings of the Ocean Drilling Program, Scientific Results, 125, pp. 445-485. College Station, TX, USA.

Jochum, K. P., Weis, U., Stoll, B., Kuzmin, D., Yang, Q., Raczek, I., Jacob, D. E., Stracke, A., Birbaum, K., Frick, D. A., Günther, D., and Enzweiler, J., 2011, Determination of Reference Values for NIST SRM 610–617 Glasses Following ISO Guidelines: Geostandards and Geoanalytical Research, v. 35, no. 4, p. 397-429.

Khedr, M., and Arai, S., 2010, Hydrous peridotites with Ti-rich chromian spinel as a low-temperature forearc mantle facies: evidence from the Happo-O'ne metaperidotites (Japan): Contributions to Mineralogy and Petrology, v. 159, no. 2, p. 137-157.

McLennan, S.M., 2001. Relationships between the trace element composition of sedimentary rocks and upper continental crust. Geochemistry, Geophysics, Geosystems, 2(4): 1021.

Nozaka, T., 2014, Metasomatic hydration of the Oeyama forearc peridotites: Tectonic implications: Lithos, v. 184-187, no. 0, p. 346-360.

Ohara, Y., and Ishii, T., 1998, Peridotites from the southern Mariana forearc: Heterogeneous fluid supply in mantle wedge: Island Arc, v. 7, no. 3, p. 541-558.

Parkinson, I. J., and Pearce, J. A., 1998, Peridotites from the Izu–Bonin–Mariana Forearc (ODP Leg 125): Evidence for Mantle Melting and Melt–Mantle Interaction in a Supra-Subduction Zone Setting: Journal of Petrology, v. 39, no. 9, p. 1577-1618.

Peccerillo, A., and Taylor, S. R., 1976, Geochemistry of eocene calc-alkaline volcanic rocks from the Kastamonu area, Northern Turkey: Contributions to Mineralogy and Petrology, v. 58, no. 1, p. 63-81.

Pearson, D. G., 1999, The age of continental roots: Lithos, v. 48, no. 1-4, p. 171-194.

Plank, T., Langmuir, C.H., 1998. The chemical composition of subducting sediment and its consequences for the crust and mantle. Chemical Geology, 145(3-4): 325-394.

Taylor, S.R., McLennan, S.M., 1995. The geochemical evolution of the continental crust. Reviews of Geophysics, 33(2): 241-265.